Iranian Journal of Chemical Engineering

Journal Homepage: www.ijche.com

pISSN: 1735-5397
eISSN: 2008-2355

Regular Article

Evaluation of the Silica Gel Adsorbent Potential for Carbon Dioxide Capture: Experimental and Modeling

Z. Koshraftar, A. Ghaemi*, H. Mashhadimoslem

School of Chemical, Petroleum and Gas Engineering, Iran University of Science and Technology, Narmak, P. O. Box: 16846, Tehran, Iran

ARTICLE INFO

Article history:
Received: 2022-04-01
Accepted: 2022-06-28
Available online: 2022-07-31

Keywords:
Carbon Dioxide,
Adsorption,
Silica Gel,
Isotherm,
Kinetics

ABSTRACT

In this research, silica gel as a low-cost adsorbent for the uptake of carbon dioxide was investigated experimentally. The samples were characterized by XRD, BET and FT-IR. It shows that as pressure was increased from 2 to 8 bar, the CO_2 adsorption capability improved over time. At a pressure of 6 bar and a dose of 1 g of silica gel, the impact of temperature (25, 45, 65, and 85 °C) on the CO_2 adsorption capacity (mg/g) was determined. The process behavior was investigated using isotherm, kinetics and thermodynamic models. As the temperature rises at a constant pressure, the adsorption capacity decreases. The experimental data of the carbon dioxide adsorption using silica gel have a high correlation coefficient with both Langmuir (0.998) and Freundlich (0.999) models. The results of the carbon dioxide adsorption kinetics with the silica gel adsorbent show that the correlation coefficient (R^2) of the second-order model and Ritchie's second model are equal to 0.995 and have the highest value. The total pore volume was 0.005119 ($cm^3\ g^{-1}$) and the specific surface area was 2.1723 ($m^2 g^{-1}$). The maximum CO_2 adsorption capacity at 25 °C near 8 bar was 195.8 mg/g.

DOI: 10.22034/ijche.2022.335792.1425 URL: http://www.ijche.com/article_154280.html

1. Introduction

Continuous emission of high levels of carbon dioxide (CO_2) into the atmosphere has a variety of significant negative effects. To prevent potentially irreversible sudden climate change, scientists have confirmed that humanity must restrict global mean temperature increases [1-5]. The annual average concentration of carbon dioxide (CO_2), the most significant anthropogenic greenhouse gas, increased to 405 and 408 parts per million (ppm) in 2017 and 2018 respectively [6]. Carbon materials and other mineral materials such as activated carbon (AC), graphene, metal-organic frameworks (MOFs), alkali metal carbonates, and zeolites

*Corresponding author: aghaemi@iust.ac.ir (A. Ghaemi)

rapidly gained popularity as CO_2 adsorbents [7, 8]. A large number of porous materials, including MCM-41, SBA-15, clays, porous silica, and others, have been mentioned in the literatures; the CO_2 adsorption on such porous materials is typically performed by physical adsorption, and thus the capacity and selectivity parameters are generally low at elevated temperatures [7-10]. A porous silica material, such as MCM-41 and SBA-15, was used as the first porous solid to produce NFSAs because of the high concentrations of silanol groups (Si-OH) on its surface, a mesoporous structure, and tunable pore size [11]. Bhagiyalakshmi et al. [12] and Su et al. [13] used rice husk ash and quartz sand as fillers to synthesize MCM-41, MCM-48, and SBA-15.

Researchers must promote the CO_2 capture technologies that are reliable, energy-efficient, cost-effective, and simple to operate, and can be used in the industrial large scales. The catalytic oxidation, sequestration, and physical and chemical adsorption are all options for CO_2 capture. The process of the separation of gas mixture by adsorption is one of the most efficient techniques of removing CO_2, and much research on CO_2 separation by adsorption has been performed in the last two decades [13-15].

Silica gel is an amorphous material, which is usually trapped in a hydrophilic matrix and adsorbs electron-deficient species readily due to its negatively charged surface [16]. Due to the water vapour adsorption potential of silica gel, water and trace impurities are frequently removed from gas mixtures [17]. Thomas et al., discussed the uptake of CO_2 on silica gel and 13X zeolite experimentally and theoretically. Helium gas was used to measure the volume of the adsorbent and the solid sections of the bed of the measurement device, which are highly effective on the adsorption temperatures. They also investigated the geometric influence of the chamber on the adsorption isotherms under supercritical circumstances using a model based on the fundamental density theory. It was originally used to explain adsorption in adsorbents with various pore size distributions. The findings of the model and the experimental data are compared, and the acceptable agreement between the two is explained [18]. Earl et al., investigated the uptake of the isotherms of carbon dioxide in the temperature range of 278-238 K at seven temperatures above 3300 kPa on two AC adsorbents and silica gel. They showed that the maximum pressure is related to the relative pressure of 0.85 P/P_s where they witnessed the capillary density. Earl et al., observed that the adsorption on AC increased sharply at low pressures, while adsorption increased slowly at high and medium pressures [19].

Table 1 summarized the different types of the gas adsorption on silica gel. It is clear that the Silica gel adsorbent was used for the adsorption of different components of gas.

Mainly in this work, the adsorption of CO_2 on silica gel as a low-cost adsorbent was investigated experimentally and theoretically. The adsorbent was characterized using a variety of techniques including FTIR, BET, and XRD.

The experiments of the adsorption CO_2 were carried out at different pressures and temperatures. The adsorption process behaviour and mechanism were investigated using isotherm, kinetic and thermodynamic models. The Clausius–Clapeyron equation was used to measure the isosteric temperatures of adsorption, and to fit the

adsorption data, the Langmuir and Freundlich's models were used.

Table 1

An overview of the adsorption equilibrium experiments and modeling.

Ref.	Adsorbent	Gas type	T (K)	P (bar)	Remark
[7]	Amine impregnated porous silica gel	CO_2	323-383	-	The adsorbent indicated CO_2 adsorption capacity at temperatures as low as 100 °C; adsorbent modified with 15 wt % PEI had CO_2 adsorption capacity of 1.16 mmol/g at 50 °C.
[17]	Silica gels	N_2O, O_2, N_2, and CO_2	293, 308, 323	10	In contrast to activated carbon, CO_2 adsorbs more strongly to silica gel than N_2O.
[19]	Activated carbon and Silica gel	CO_2	273-373	40	Using this automated instrument, the researcher can measure isotherms of adsorption at pressures up to 3350 kPa.
[20]	Amine-functionalized mesoporous silica	CO_2	313	1	The adsorption kinetics showed that the CO_2 capture was impressed by kinetic and thermodynamic to different extents depending on the adsorption temperature.
[21]	Polyethyleneimine modified silica gel	CO_2	298.15, 308.15 and 318.15	0.667	With a high adsorption capacity at 298.15 K, the smaller-particle (15μm) PEI-modified silica gel exhibited the most ability to adsorb.
[22]	Silica gel	N_2 and CO_2 and their mixture	298, 313, 333	1-3	Transport of CO_2/N_2 mixture in silica gel pores is well captured by the mechanism established from the single component study.
[23]	Calixarene compounds immobilized on silica gel	CO_2, CH_4 and N_2	298, 283, 313	0-30	Amino functionalized Calix-Silica showed high CO_2 selectivity over N_2 and CH_4.
[24]	Silica-APTES aerogel	CO_2/CH_4	293	90-120	As pressure increases, CO_2's adsorption capacity increases.
[25]	Amine-based silica aerogels	CO_2	-	-	CO_2 adsorption capacities of aerogels increased with the addition of ionic liquid.
[26]	Silica gel	CO_2	288-318	0-5	Experimental and theoretical studies have been conducted on silica gel for CH_4 and CO_2.
[27]	Amino functionalised silica aerogels	CO_2	273	0.0025	Two aminosilanes applied for silica aerogel functionalisation & adsorbent generation.
[28]	silica-based adsorbents from TFT-LCD industrial waste powder	CO_2	298	1	Mesoporous silica, MSPs (HNO_3) fabricated from TFT-LCD waste can be a cost-effective CO_2 adsorbent.

[29]	Amines immobilized double-walled silica nanotubes	CO_2	298, 323, 348, 373	1	This study indicates the amine type apt for the CO_2 capture. The CO_2 capture capacity of adsorbents decreased linearly with the increase of the adsorption temperature.
[30]	Silica aerogel immobilized with tetraethylenepentamine	CO_2	348	1	Aerogel sorbents have a significant CO_2 adsorption capability.
This work	Silica gel	CO_2	298, 318, 338, 358	2-8	Silica gel uptake experiments were well fitted by second-order and Ritchie's second model.

2. Materials and methods

Silica gel granules purchased from BOSF (Germany) company. Silica gel granules was crushed and sieved with mesh size in the range of 0.2-0.5 mm. A gas flow of CO_2 with the purity of 99.99 % was used that provided by Sabalan Gas Company of Tehran (Iran). The International Union of Pure and Applied Chemistry (IUPAC) suggested pore size classification (Sing et al., 1985) is frequently used to define the pore size range (Micropores d < 2 nm; Mesopores 2 < d < 50 nm; Macropores d > 50 nm). There are a few adsorbents that have a strong affinity for water [31]. Silica gel pellets were crushed and sieved (0.2-0.5 mm). Silica gel is a popular mineral material in industrial applications for the adsorption process. Silica gel is hydrophilic and has a high porosity level. Silica gels are made from the crystalline or amorphous tridymite, cristobalite, and quartz. Silica gel has hydrated amorphous silica ($SiO_2.nH_2O$) in its chemical composition, and it is formed by polycondensation. Its internal structure consists of a large network of interconnected microscopic cavities. The surface of the silica gel consists of Si-OH and Si-O-Si groups and is polar. Due to the presence of Si-OH on the surface, silica gels have remarkable surface and chemical properties. As shown in Figure1, OH groups mainly occupy the outer quadrangular vertices on the surface of the silica gel, and the cavities also form small internal slits. Among silica-based materials, silicon dioxide gel with the general formula of $SiO_2.xH_2O$ is studied primarily for its ability to absorb water [32].

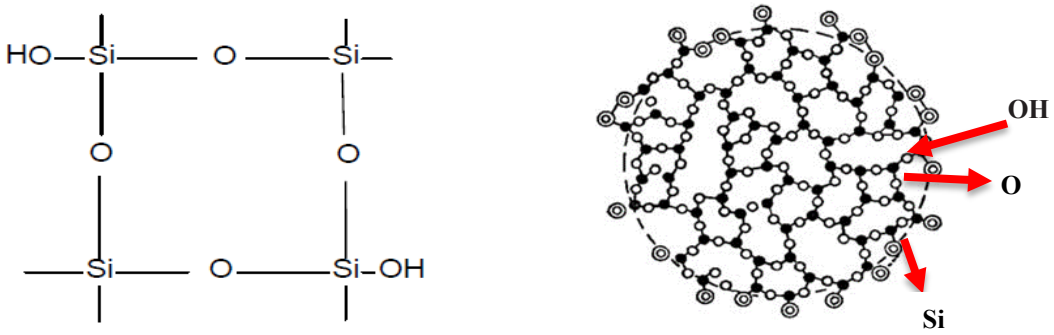

Figure 1. Structure of silica gel globules.

Figure 2 depicts a schematic and visual representation of the experimental apparatus used to assess the CO_2 adsorption capacity. The fixed reactor is made of stainless steel

(volume 254.34 cm^3), pure gas capsule CO_2, pressure and gas regulating valves, heater, mixing tank, barometer, and a digital display. The reactor can control the main variables, such as temperature, and pressure, which affect the removal of carbon dioxide from the air. In the beginning of each experiment temperature and pressure are set to specific values. The materials used in the experiment were placed in a reactor cell. The initial pressure of CO_2 is controlled by a pressure monitor and valves linked to the reactor that allows pure CO_2 to enter the reactor. The absorption begins after adjusting the pressure and temperature. The adsorption data was stored during one hour.

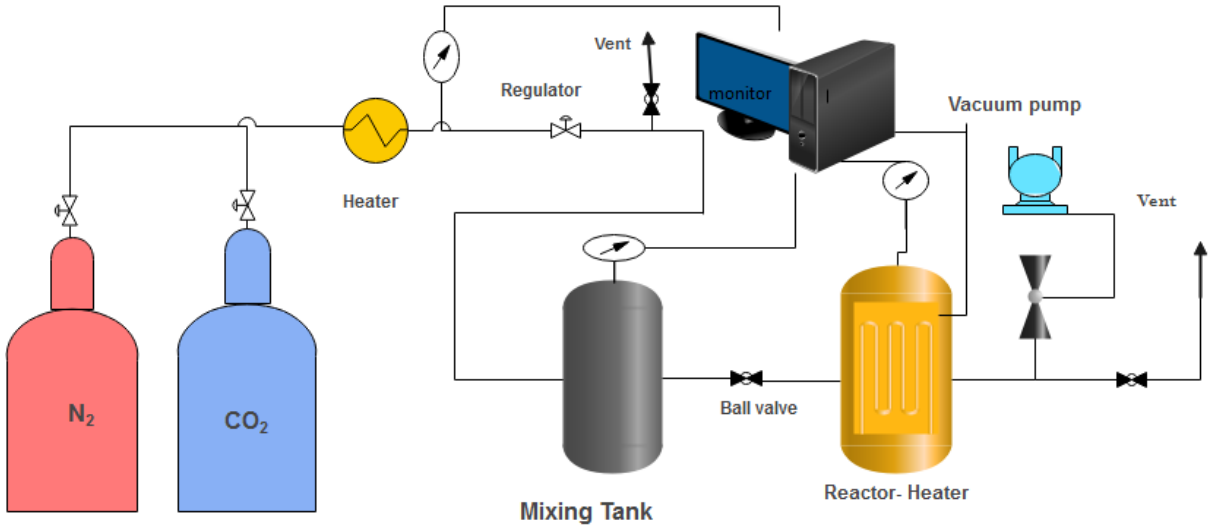

Figure 2. Schematic of a fixed bed surface adsorption equipment.

For each test, 1 gram of the produced silica gel, as described in part in the Materials and methods section, is entered into the tank. After the device temperature and pressure have been configured, the adsorption prosess was started. The instrument is allowed an hour to finish the adsorption process. The percentage of adsorption, as well as the capacity, were shown. The percentage of adsorption and capacity were presented [3]:

$$\text{adsorption}(\%)=\frac{P_i-P_f}{P_i}\times 100 \quad (1)$$

$$q_e=\frac{(p_{i-p_e})VM_{CO2}}{RTm}\times 1000 \quad (2)$$

The correlation coefficient (R^2) (Eq. (3)) can be used to assess how well the kinetic and isotherm models match the experimental results [3].

$$R^2=\frac{\left(q_{e,meas}-\overline{q_{e,calc}}\right)^2}{\sum\left(q_{e,meas}-\overline{q_{e,calc}}\right)^2+\left(q_{e,meas}-q_{e,calc}\right)^2} \quad (3)$$

3. Adsorbent characterization

FTIR spectroscopy data were obtained in the range of 4000-400 (cm^{-1}) using a Fourier transformed-infrared 8400 Spectrometer (Shimadzu Corporation, Japan). The laboratory FTIR system is an infrared Fourier transform spectrometer made by Vertex Company with German model 70 and can

measure the passage and absorption spectra of liquid, solid, and powder samples. For infrared spectroscopy, the sample is prepared in the form of a tablet and placed in the equipment [33]. The chemical composition and crystalline characteristics of rocks, ceramics, metals, and synthetic materials are determined using X-ray diffraction spectroscopy, which is frequently utilized in engineering. Each crystal has its own X-ray pattern [34]. Qualitative and quantitative diffraction measurements are performed using X 'Pert High Score software (Model: STOE STADI-MP Germany; Radiation: Cu-Kα; Voltage: 40kV; 30 mA). A BET diagram is a linear diagram from which the specific or effective surface area of a substance is extracted [35]. The effective surface area of a substance is expressed in square meters per gram. One of the characteristics of intermediate or porous materials is having a large area. The isotherms of the nitrogen adsorption/desorption at 77 K are measured on an ASAP 2020 adsorption system from Micromeritics [2]. Each sample was evacuated and reduced to 180 °C for more than 6 hours under high vacuum conditions before measurement. The particle size distribution (PSD) is calculated by the nonlinear density function comparative method using nitrogen adsorption data [2].

4. Results and discussion

4.1. Structures of the silica gel sorbent

Figure 3 indicates the FTIR spectra of silica gel. The peaks at 480-500 (cm^{-1}), correspond to Si-O groups. Near 800 (cm^{-1}), the bands related to the stretching vibration mode of Si-O-Si are observed [35]. The apparent peak in the range 1000-1250 (cm^{-1}) is related to Si-O groups. H_2O peaks can be seen at 1750 (cm^{-1}) and also in the ranges of 3250-3500 cm^{-1}. Finally, at point 3750 (cm^{-1}), O-H group is observed. The orange diagram is the silica gel spectroscopy diagram before the uptake of carbon dioxide, and the blue diagram is the silica gel spectroscopy diagram after the uptake of carbon dioxide. As it can be seen, the silica gel peaks have expanded after the CO_2 adsorption compared to before the gas adsorption. Table 2 discusses the functional groups in silica gel structure.

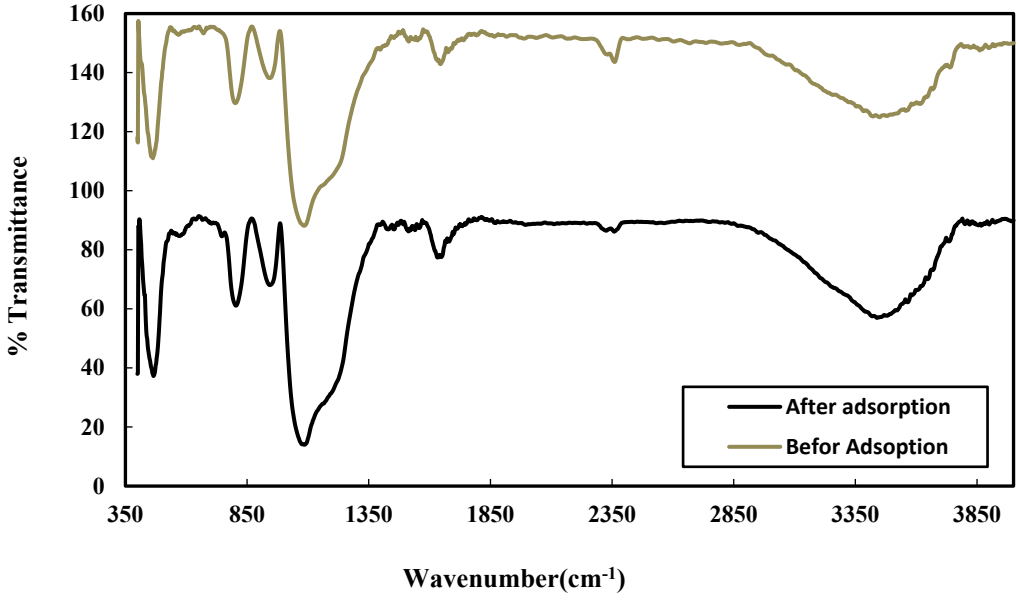

Figure 3. FTIR of silica gel.

Table 2
FTIR spectral characteristics of silica gel.

Frequency (cm^{-1})	Position assignment	Previously reported value (cm^{-1})	References
485	Si–O bond rocking	465-500	[16]
850	OH bending (silanol)	800–870	[16]
975	Si–OH bond stretching	935–980	[16]
1250	Asymmetric Si–O–Si stretching	1050–1150	[16]
3750	O–H stretching	3740-3750	

The crystalline structure of the adsorbent and its phases were investigated using X-ray diffraction. Figure 4 shows the XRD pattern of silica gel. The dispersion peaks related to silica gel adsorbents, especially in the range of 15 to 35, can be seen in Fig. 4. Despite the lack of sharp peaks, the silica contains no crystalline content [36]. The XRD pattern of the amorphous material has a long peak between 15 and 35 degrees of Bragg angle 2. An amorphous peak was detected at the Bragg angle of 2θ = 23 degrees in the large peak noted in the XRD pattern, which is the same as that produced by a sol-gel procedure for obtaining amorphous silica [37]. The peak with a broad range of 2θ also shows that the silica generated by low-temperature vapour-phase hydrolysis technique is amorphous. The previous findings were in strong agreement with the XRD study results. The diffraction patterns are identical without any crystalline peaks, indicating that silica materials are non-crystalline [37].

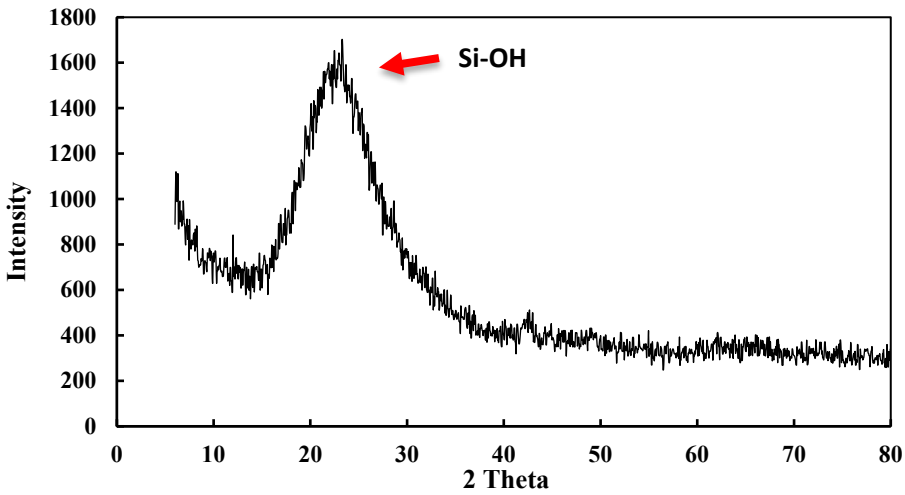

Figure 4. XRD patterns of silica gel.

Figures 5 and 6 show the adsorption/desorption of N_2 and the pore size distribution of silica gel. Table 3 indicates the structural properties (Total pore volume, specific surface area, pore diameter, pore volume) of silica gel. According to IUPAC classification, type IV isotherms are the characteristic of systems containing mesoporous pores because they exhibit a strong interaction between N_2 and silica gel, which results in a steep increase in the isotherm under low partial pressures [3]. The total pore volume was 0.005119 ($cm^3\ g^{-1}$) and the specific surface area (S_{BET}) was 2.1723

(m^2g^{-1}). The isotherm also revealed that the material had a mesoporous system with a hysteresis loop that appeared at high relative pressures [39, 40]. The pattern, however, is consistent with a form IV isotherm beyond a certain P/P_0 value, suggesting a normal mesoporous structure [38]. For the pore size analysis, the Barret-Joyner-Halenda (BJH) equilibrium model was used. In Figure 6, the pore diameters of silica gel is observed.

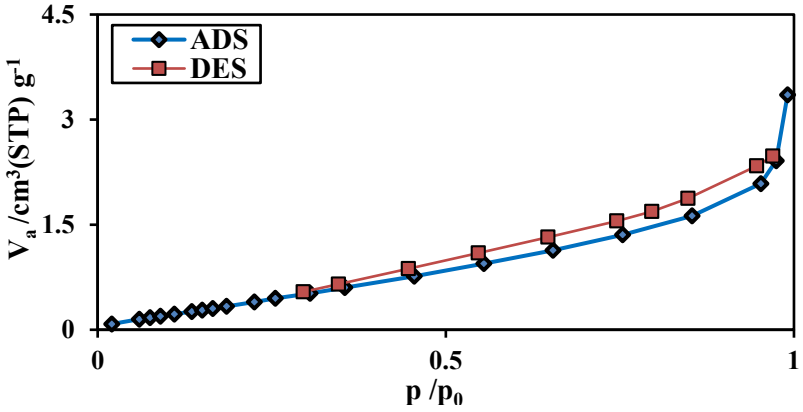

Figue 5. N_2 adsorption / desorption isotherm on silica gel at 77 K.

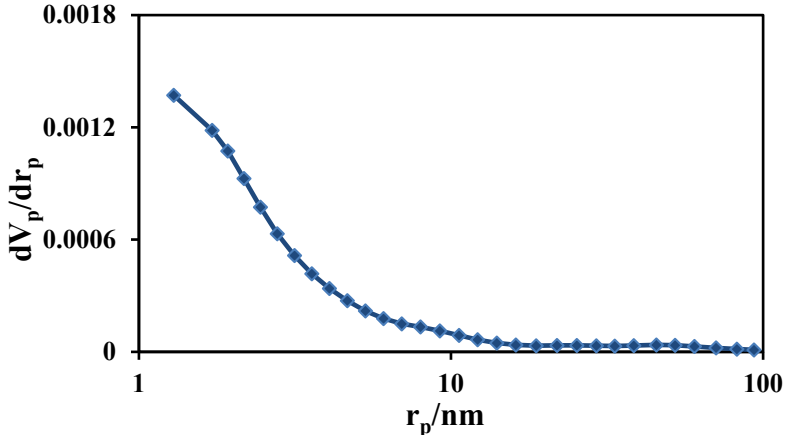

Figure 6. Distribution of the pore size of silica gel by the BJH method according to pore area.

Table 3

The structural properties of the silica gel.

BET-plot	V_m [cm^3(STP) g^{-1}]	$a_{s,BET}$ [m^2 g^{-1}]	Total pore volume ($p/p_0 = 0.990$) [cm^3 g^{-1}]	Mean pore diameter [nm]
	0.4991	2.1723	0.005119	9.426
Langmuir plot	V_m [cm^3(STP) g^{-1}]		$a_{s,Lang}$ [m^2 g^{-1}]	
	0.3688		1.6052	
t-plot	Plot data a_1		Plot data V_1	
	0.51		0	
BJH-plot	Plot data V_p [cm^3 g^{-1}]	Plot data $r_{p,peak}$ (Area) [nm]	Plot data a_p [m^2 g^{-1}]	
	0.0059775	1.29	3.2143	

4.2. Effect of pressure

Furthermore, according to the data gathered from the research on the influence of pressure on the carbon dioxide adsorption by silica gel, the intensity of the gas adsorption rises by increasing pressure (Figure 7). It shows that as pressure was increased from 2 to 8 bar, the CO_2 adsorption capability improved over time [3]. Figure 8 shows the 3D curves of the combined influence of temperature and time on the CO_2 adsorption efficiency. As a result, raising pressure has a direct effect on the CO_2 adsorption capacity. The adsorbent has a maximum CO_2 (195.8 mg/g) adsorption capacity of near 8 bar.

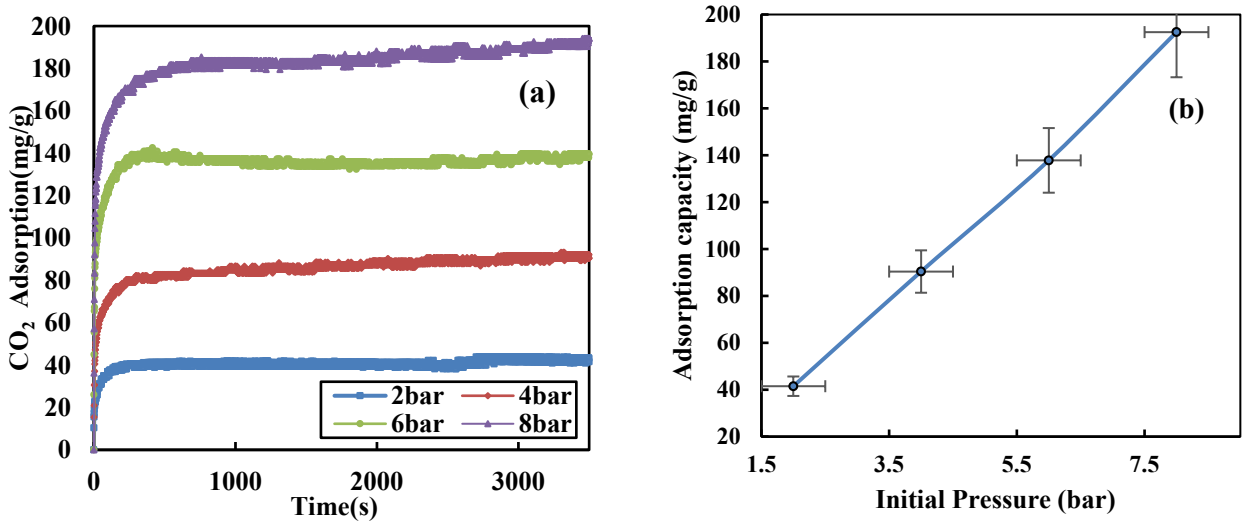

Figure 7. Adsorption capacity of CO_2 as a function of pressure at 25 °C during the time (a) and, the adsorption capacity of CO_2 with respect to pressure (b).

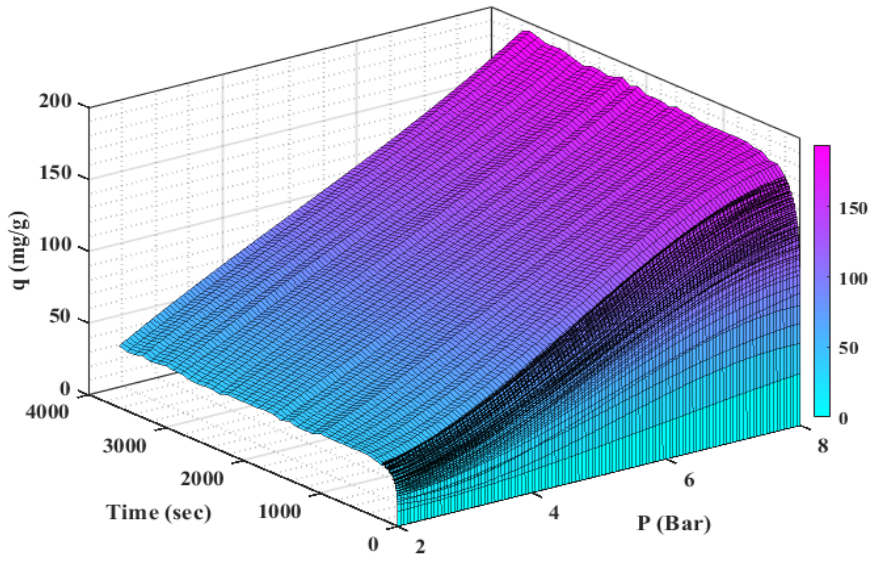

Figure 8. 3-D curve effect of pressure on the CO_2 adsorption capacity at 25 °C during the time.

4.3. Effect of temperature

At a pressure of 6 bar and a dose of 1g of silica gel, the impact of temperature (25, 45, 65, and 85 °C) on the CO_2 adsorption

capacity (mg/g) was determined (Figure 9). The absorption intensity reduces as the temperature rises at a constant pressure. Furthermore, Figure 10 shows the 3D curves of the combined influence of temperature and time on the CO_2 adsorption efficiency. As it can be seen, increasing the temperature from 25 to 85 °C lowered the CO_2 adsorption capacity of the adsorbent, with the greatest value of the CO_2 adsorption capacity occurring at 25 °C. The results show that the CO_2 adsorption process is extremely exothermic, and that raising the temperature reduces the uptake capability of CO_2.

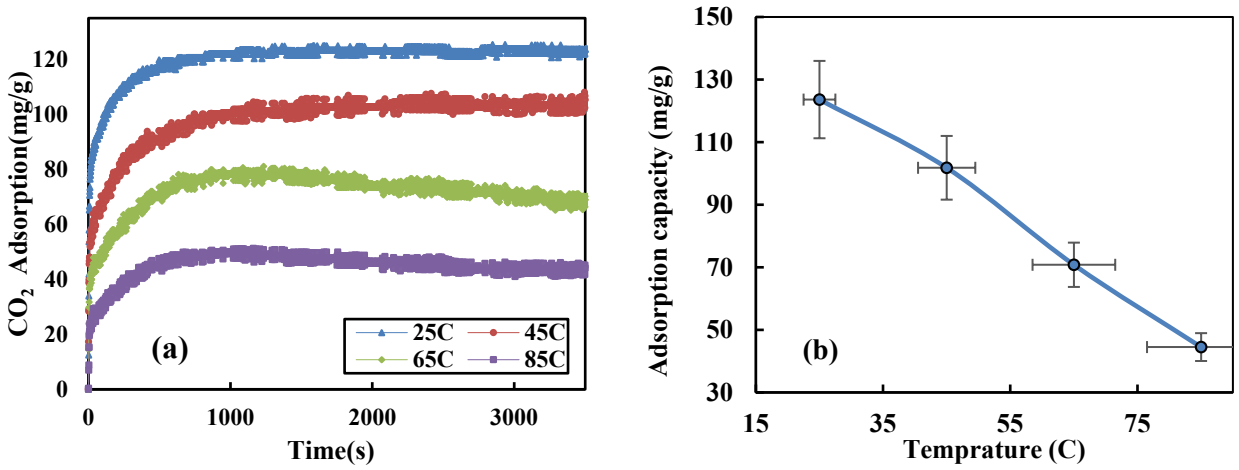

Figure 9. Adsorption capacity of CO_2 as a function of temperature at 6 bar during time (a) and, the adsorption capacity of CO_2 with respect to temperature (b).

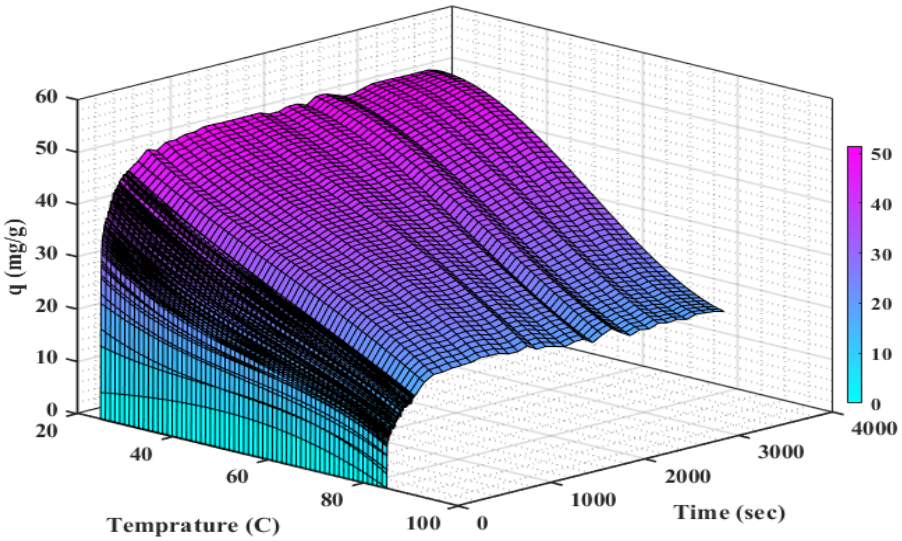

Figure 10. 3-D curve: An investigation of the impact of pressure on the CO_2 adsorption capacity at 25 °C during time.

4.4. Isotherm modeling

The Langmuir-Freundlich models are concerned with the low-temperature adsorption. As a result, they are suited for physical adsorptions. The Loshatelia principle explains the decrease in the CO_2 adsorption capability. As a result, at high temperatures, desorption is desired. The carbon dioxide

adsorption is inversely proportional to the value of q_m, which tends to decrease as the adsorption temperature rises. The separation factor R indicates the desirability of the adsorption method. At various temperatures and pressures, R_L is computed. The value of R_L is in the range of 0-1, the closer this value is to one, the more desirable the absorption of carbon dioxide. The obedience and R-D isotherms provide useful information about energy variables. In these models, E is the free energy of absorption and b_T is the heat of absorption. If E < 8 (kJ/mol) it is physical adsorption and if it is 8< E < 16 (kJ/mol) it is chemical adsorption [41]. The Langmuir model is the best description of a chemical reaction due to its confinement to one layer. Freundlich, on the other hand, primarily represents the process of physical absorption. A value of n_f < 1 (Freundlich) indicates that the uptake of CO_2 on the adsorbent is a chemical process. However, if the value is n_f > 1, adsorption will be a physical process. High n values indicate an active site with high energy.

The experimental data presented in Table (4) are of the carbon dioxide adsorption using silica gel and have a high correlation coefficient with both the Langmuir (0.998) and Freundlich (0.999) models. For the physical adsorption, the Langmuir model is appropriate, whereas the Freundlich model is appropriate for the chemical adsorption, if its variable is less than 1. Since the value of the obtained variable n is equal to 0.78 and less than 1, the adsorption is considered chemical, but since the inverse of the variable n is greater than 1, this adsorption is undesirable. The resulting diagram is presented in Figure 11.

Table 4
Kinetic variables of the CO_2 adsorption isotherm using silica gel at 25 °C.

Models	Parameter	Values
Langmuir : $q_e=\frac{q_m k_L P_e}{(1+k_L P_e)}$	q_m	92148.290
	K_L	0.00001
	R^2	0.9983
Freundlich : $q_e=k_F P^{1/n}$	k_F	15.316
	n	0.786
	R^2	0.9998
Dubinin Radushkevich : $q_e=q_m e^{-\lambda\omega^2}$	q_m	239.896
	beta	2.844
	E	0.419
	R^2	0.9682

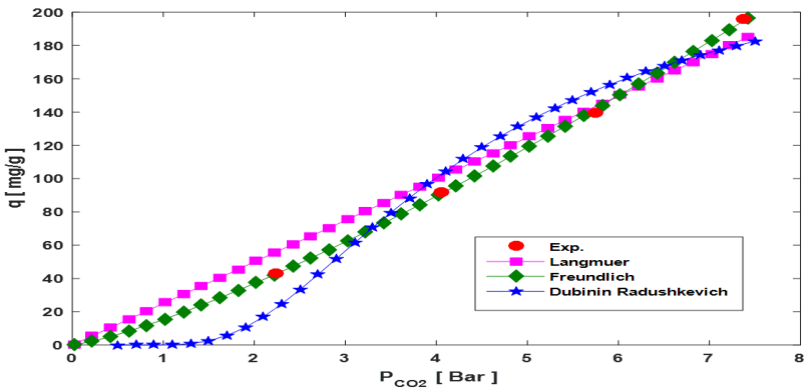

Figure 11. Kinetic modelling for the CO_2 adsorption on silica gel at 6 bar.

4.5. Kinetic and Thermodynamic modeling

One of the most important criteria that impacts the adsorption effectiveness is adsorption kinetics [42]. The results of the carbon dioxide adsorption kinetics with the silica gel adsorbent shown in Figure (12) show that the correlation coefficient (R^2) of the second-order model and Ritchie second model are equal to 0.996 and have the highest value. It is most consistent with the experimental data and therefore the controlling agent of the chemical adsorption process. Kinetic data are presented in Table 5.

Table 5

Kinetic variables of the carbon dioxide adsorption using the silica gel adsorbent.

Models	Parameter	25 °C	45 °C	65 °C	85 °C
First order model: $q_t=q_e\left(1-e^{(-k_f t)}\right)$	q_e	121.670	101.360	73.494	46.127
	k_f	0.01821	0.00884	0.00968	0.00968
	R^2	0.9748	0.9529	0.9375	0.9391
Second order model: $q_t=\frac{q_e^2 k_s t}{1+q_e k_s t}$	q_e	124.394	105.525	75.422	47.277
	k_s	0.00031	0.00016	0.00032	0.00053
	R^2	0.9959	0.9913	0.9377	0.9306
Ritchie second model: $q_t=q_e\left(1-1-\left[\frac{q_e}{(1+k_2 t)}\right]\right)$	q_e	124.394	105.525	75.422	47.277
	k_2	0.03850	0.01689	0.02430	0.02501
	R^2	0.9959	0.9913	0.9377	0.9306

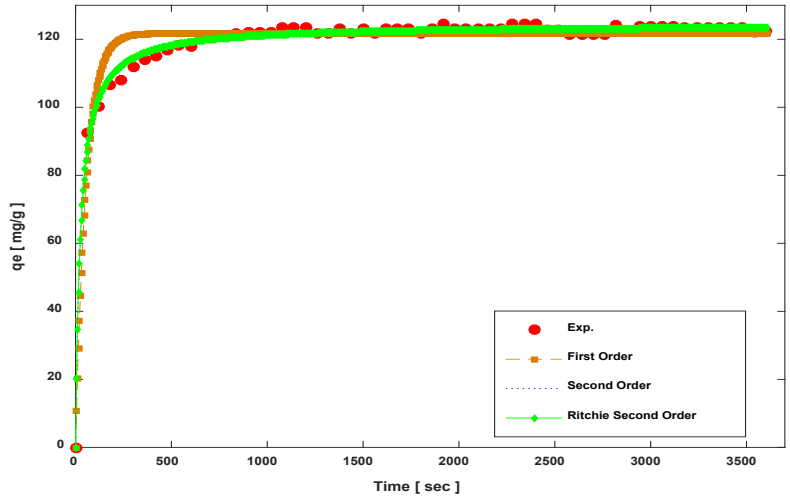

Figure 12. Kinetic diagram of the uptake of carbon dioxide using silica gel at 25 °C.

The Gibbs free energy of adsorption (ΔG°), the Enthalpy change (ΔH°), and the entropy change (ΔS°) are conducted to understand how the thermodynamic processes operate. The ΔG° is an indication of the spontaneity of an adsorption and therefore is one of the most important criteria. It is calculated in the following way: [43]:

$$\Delta G^{o}=-RT\ln K_D \quad (4)$$

$$\Delta G^{o}=\Delta H^{o}-T\Delta S^{o} \quad (5)$$

$$\ln K_D=\frac{\Delta S^{o}}{R}-\frac{\Delta H^{o}}{RT} \quad (6)$$

The value of ΔH° is positive and this indicates that the carbon dioxide adsorption using silica gel is an endothermic process. The adsorption process is not spontaneous since ΔS° is negative and ΔG° is positive. The value of ΔS° is negative, indicating that the adsorption mechanism is becoming less irregular [44, 45]. As a result, adsorbate molecules are found at specific adsorbent sites, and the adsorbent molecules are regularly arranged. Silica gel has a better adsorption capacity at low temperatures. The thermodynamic diagrams and carbon dioxide adsorption data using silica gel are presented in Figure (13) and Table (6) respectively.

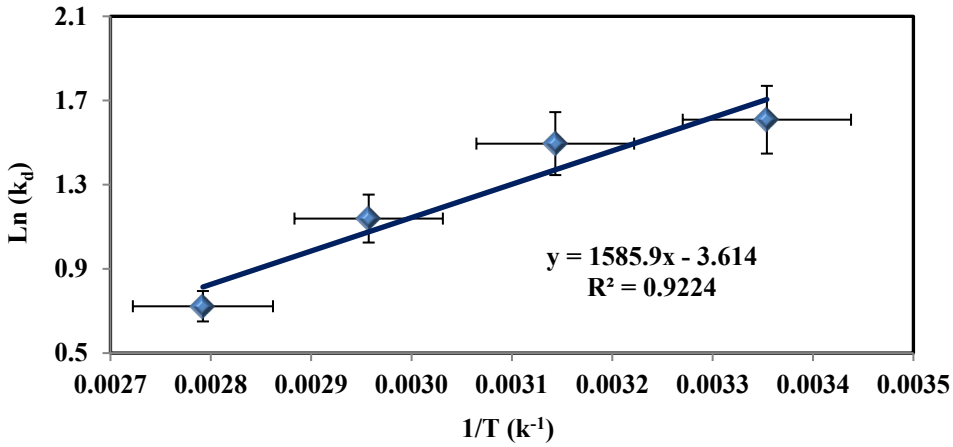

Figure 13. Plot of Ln k_d versus 1/T for the adsorption of CO_2 on Silica gel.

Table 6
Kinetic variables of the CO_2 adsorption using silica gel adsorbent.

P (bar)	ΔH (kJ/mol)	ΔS (kJ/mol.K)	ΔG (kJ/mol)		
			45 °C	65 °C	85 °C
6	13.186	-0.030	22.746	23.347	23.948

5. Conclusions

In this study, the adsorption of CO_2 was analyzed with the silica gel adsorbent. The uptake of carbon dioxide via silica gel was investigated by examining variables such as the temperature (25 to 85 °C) and pressure (2 to 8 bar) which is a novelty of this work. The investigation of the kinetic and thermodynamic modeling in this range of temperature is another novelty of this work. About the temperature variable, the adsorption rate of this gas decreases by increasing temperature and about the pressure variable, the adsorption rate increases. Several instrumentation tools such as FTIR, BET, and XRD were applied to characterize the silica gel. Its specific surface area (S_{BET}) was 2.1723 (m^2g^{-1}) and its total pore volume was 0.005119 (cm^3 g^{-1}). The XRD pattern includes an amorphous peak identified at Bragg angle of 2θ = 23 degrees. The diffraction patterns are identical without any crystalline peaks, indicating that silica materials are non-crystalline. Langmuir and Freundlich were found the best fit in most situations, signifying the monolayer uniform adsorption. A value of $n_f < 1$ (Freundlich) indicates that the uptake of CO_2 on the adsorbent is a chemical process. The isotherm also revealed that the material had a

mesoporous system with a hysteresis loop that appeared at high relative pressure. According to kinetic modeling, the values of R^2 showed that the kinetic data followed the pseudo-second-order (PSO) model. In thermodynamic studies, since ΔS° and ΔG° did not have the same sign, the adsorption process by silica gel was not spontaneous. The silica gel adsorbent has a maximum CO_2 (195.8 mg/g) uptake capacity near 8 bar at 25 °C. Silica gel has very appealing properties such as low-cost, non-toxicity, and environmentally friendly adsorbent for using the CO_2 adsorption.

Acknowledgement

The authors wish to thank the management of the School of Chemical, Petrolieum and Gas Engineering at Iran University of Science and Technology for providing the necessary support.

References

[1] Taheri, F. S., Ghaemi, A., Maleki, A. and Shahhosseini, S., "High CO_2 adsorption on amine-functionalized improved mesoporous silica nanotube as an eco-friendly nanocomposite", *Energy & Fuels*, **33**, 5384-5397 (2019).

[2] Khoshraftar, Z. and Ghaemi, A., "Presence of activated carbon particles from waste walnut shell as a biosorbent in monoethanolamine (MEA) solution to enhance carbon dioxide absorption", *Heliyon*, **8**, e08689 (2022).

[3] Khoshraftar, Z., Ghaemi, A. and Sigaroodi, A. H. M., "The effect of solid adsorbents in Triethanolamine (TEA) solution for enhanced CO_2 absorption rate", *Res. Chem. Intermed.*, **47**, 43 (2021).

[4] Naeem, S., Ghaemi, A. and Shahhosseini, S., "Experimental investigation of CO_2 capture using sodium hydroxide particles in a fluidized bed", *Korean J. Chem. Eng.*, **33**, 1278 (2016).

[5] Pashaei, H., Ghaemi, A., Nasiri, M. and Karami, B., "Experimental modeling and optimization of CO_2 absorption into piperazine solutions using RSM-CCD methodology", *ACS Omega*, **5**, 8432 (2020).

[6] Li, K., Jiang, J., Tian, S., Yan, F. and Chen, X., "Polyethyleneimine-nano silica composites: A low-cost and promising adsorbent for CO_2 capture", *J. Mater. Chem. A*, **3**, 2166 (2015).

[7] Minju, N., Abhilash, P., Nair, B. N., Mohamed, A. P. and Ananthakumar, S., "Amine impregnated porous silica gel sorbents synthesized from water-glass precursors for CO_2 capturing", *Chem. Eng. J.*, **269**, 335 (2015).

[8] Nair, B. N., Burwood, R. P., Goh, V. J., Nakagawa, K. and Yamaguchi, T., "Lithium based ceramic materials and membranes for high temperature CO_2 separation", *Prog. Mater. Sci.*, **54**, 511 (2009).

[9] Chew, T.-L., Ahmad, A. L. and Bhatia, S., "Ordered mesoporous silica (OMS) as an adsorbent and membrane for separation of carbon dioxide (CO_2)", *Adv. Colloid Interface Sci.*, **153**, 43 (2010).

[10] Liu, X., Li, J., Zhou, L., Huang, D. and Zhou, Y., "Adsorption of CO_2, CH_4 and N_2 on ordered mesoporous silica molecular sieve", *Chem. Phys. Lett.*, **415**, 198 (2005).

[11] Hu, X. E., Liu, L., Luo, X., Xiao, G., Shiko, E., Zhang, R., Fan, X., Zhou, Y., Liu, Y. and Zeng, Z., "A review of N-

functionalized solid adsorbents for post-combustion CO_2 capture", *Appl. Energy*, **260**, 114244 (2020).

[12] Bhagiyalakshmi, M., Yun, L. J., Anuradha, R. and Jang, H. T., "Synthesis of chloropropylamine grafted mesoporous MCM-41, MCM-48 and SBA-15 from rice husk ash: Their application to CO_2 chemisorption", *J. Porous Mater.*, **17**, 475 (2010).

[13] Su, Y., Peng, L., Shiue, A., Hong, G. -B., Qian, Z. and Chang, C. -T., "Carbon dioxide adsorption on amine-impregnated mesoporous materials prepared from spent quartz sand", *J. Air & Waste Manag. Assoc.,* **64**, 827 (2014).

[14] Penchah, H. R., Ghaemi, A. and Gilani, H. G., "Efficiency increase in hypercrosslinked polymer based on polystyrene in CO_2 adsorption process", *Polym. Bull.*, **79**, 3681 (2022).

[15] Fashi, F., Ghaemi, A. and Moradi, P., "Comparison of improvement efficiency of alumina and zeolite using piperazine solution for carbon dioxide adsorption", *Nashrieh Shimi va Mohandesi Shimi Iran*, **39** (2), 99 (2020).

[16] Parida, S. K., Dash, S., Patel, S. and Mishra, B. K., "Adsorption of organic molecules on silica surface", *Adv. Colloid Interface Sci.*, **121**, 77 (2006).

[17] Park, D., Hong, S. -H., Kim, K. -M. and Lee, C. -H., "Adsorption equilibria and kinetics of silica gel for N_2O, O_2, N_2, and CO_2", *Sep. Purif. Technol.*, **251**, 117326 (2020).

[18] Hocker, T., Rajendran, A. and Mazzotti, M., "Measuring and modeling supercritical adsorption in porous solids. Carbon dioxide on 13X zeolite and on silica gel", *Langmuir,* **19**, 1254 (2003).

[19] Berlier, K. and Frere, M., "Adsorption of CO_2 on microporous materials. 1. On activated carbon and silica gel", *J. Chem. & Eng. Data*, **42**, 533 (1997).

[20] Henao, W., Jaramillo, L. Y., López, D., Romero-Sáez, M. and Buitrago-Sierra, R., "Insights into the CO_2 capture over amine-functionalized mesoporous silica adsorbents derived from rice husk ash", *J. Environ. Chem. Eng.*, **8**, 104362 (2020).

[21] Zhu, T., Yang, S., Choi, D. K. and Row, K. H., "Adsorption of carbon dioxide using polyethyleneimine modified silica gel", *Korean J. Chem. Eng.*, **27**, 1910 (2010).

[22] Goyal, P., Purdue, M. J. and Farooq, S., "Adsorption and diffusion of N_2 and CO_2 and their mixture on silica gel", *Ind. & Eng. Chem. Res.*, **58**, 19611 (2019).

[23] Taghizadeh, F., Mokhtarani, B., Zadmard, R. and Jalali, M. R., "Highly selective CO_2 uptake in Calix arene compounds immobilized on silica gel", *Chem. Eng. J.*, **417**, 128115 (2021).

[24] Oliveira, R. J., de Conto, J. F., Oliveira, M. R., Egues, S. M. S., Borges, G. R., Dariva, C. and Franceschi, E., "CO_2/CH_4 adsorption at high-pressure using silica-APTES aerogel as adsorbent and near infrared as a monitoring technique", *J. CO_2 Util.*, **32**, 232 (2019).

[25] Garip, M. and Gizli, N., "Ionic liquid containing amine-based silica aerogels for CO_2 capture by fixed bed adsorption", *J. Mol. Liq.*, **310**, 113227 (2020).

[26] Shen, Y., Shi, W., Zhang, D., Na, P. and Fu, B., "The removal and capture of CO_2 from biogas by vacuum pressure swing process using silica gel", *J. CO_2 Util.*, **27**, 259 (2018).

[27] Wörmeyer, K. and Smirnova, I.,

"Adsorption of CO_2, moisture and ethanol at low partial pressure using aminofunctionalised silica aerogels", *Chem. Eng. J.*, **225**, 350 (2013).

[28] Lin, L. -Y. and Bai, H., "Facile and surfactant-free route to mesoporous silica-based adsorbents from TFT-LCD industrial waste powder for CO_2 capture", *Microporous mesoporous Mater.*, **170**, 266 (2013).

[29] Ko, Y. G., Lee, H. J., Oh, H. C. and Choi, U. S., "Amines immobilized double-walled silica nanotubes for CO_2 capture", *J. Hazard. Mater.*, **250**, 53 (2013).

[30] Linneen, N., Pfeffer, R. and Lin, Y. S., "CO_2 capture using particulate silica aerogel immobilized with tetraethylenepentamine", *Microporous Mesoporous Mater*., **176**, 123 (2013).

[31] Suzuki, M., Adsorption engineering, Kodansha, Tokyo, (1990).

[32] Fomkin, A. A., "Nanoporous materials and their adsorption properties", *Prot. Met. Phys. Chem. Surfaces*, **45**, 121 (2009).

[33] Li, Z., Zhong, D. -L., Lu, Y. -Y., Wang, J. -L., Qing, S. -L. and Yan, J., "Enhanced separation of carbon dioxide from a CO_2 + CH_4 gas mixture using a hybrid adsorption-hydrate formation process in the presence of coal particles", *J. Nat. Gas Sci. Eng.*, **35**, 1472 (2016).

[34] Hartono, A., Ciftja, A. F., Brúder, P. and Svendsen, H. F., "Characterization of amine-impregnated adsorbent for CCS post combustion", *Energy Procedia*, **63**, 2138 (2014).

[35] Espínola, J. G. P., Arakaki, L. N. H., de Oliveira, S. F., da Fonseca, M. G., Campos Filho, J. A. A. and Airoldi, C., "Some thermodynamic data of the energetics of the interaction cation-piperazine immobilized on silica gel", *Colloids Surfaces A Physicochem. Eng. Asp.*, **221**, 101(2003).

[36] Utama, P. S., Yamsaengsung, R. and Sangwichien, C., "Production and characterization of precipitated silica from palm oil mill fly ash using CO_2 impregnation and mechanical fragmentation", *Brazilian J. Chem. Eng.*, **36**, 523 (2019).

[37] Chen, X., Jiang, J., Yan, F., Tian, S. and Li, K., "A novel low temperature vapor phase hydrolysis method for the production of nano-structured silica materials using silicon tetrachloride", *RSC Adv.*, **4**, 8703 (2014).

[38] Meng, Z., Liu, Y., Li, X. and Ma, Z., "Removal of siloxane (L2) from biogas using methyl-functionalised silica gel as adsorbent", *Chem. Eng. J.*, **389**, 124440 (2020).

[39] Nguyen, H. K. D., Hoang, P. T. and Dinh, N. T., "Synthesis of modified silica aerogel nanoparticles for remediation of vietnamese crude oil spilled on water", *J. Braz. Chem. Soc.*, **29**, 1714 (2018).

[40] Sneddon, G., Ganin, A. Y. and Yiu, H. H. P., "Sustainable CO_2 adsorbents prepared by coating chitosan onto mesoporous silicas for large-scale carbon capture technology", *Energy Technol.,* **3**, 249 (2015).

[41] Langmuir, I., "The constitution and fundamental properties of solids and liquids. Part I. Solids", *J. Am. Chem. Soc.*, **38**, 2221 (1916).

[42] Saeidi, M., Ghaemi, A. and Tahvildari, K., "CO_2 capture exploration on potassium hydroxide employing response surface methodology isotherm and kinetic models", *Iran. J. Chem. Chem.*

Eng., **39**, 255 (2020).

[43] Saeidi, M., Ghaemi, A., Tahvildari, K. and Derakhshi, P., "Exploiting response surface methodology (RSM) as a novel approach for the optimization of carbon dioxide adsorption by dry sodium hydroxide", *J. Chinese Chem. Soc.*, **65**, 1465 (2018).

[44] Ghaemi, A., Mashhadimoslem, H. and Zohourian Izadpanah, P., "NiO and MgO/activated carbon as an efficient CO_2 adsorbent: characterization, modeling, and optimization", *Int. J. Environ. Sci. Technol.,* **19**, 727 (2022).

[45] Mashhadimoslem, H., Safarzadeh, M., Ghaemi, A., Emrooz, H. B. M. and Barzegar, M., "Biomass derived hierarchical porous carbon for high-performance O_2/N_2 adsorption; A new green self-activation approach", *RSC Advances*., **11** (57), 36125 (2021).